SURFACE AND INTERFACE ANALYSIS
Surf. Interface Anal. 2002; **33**: 351–360
Published online in Wiley InterScience (www.interscience.wiley.com). DOI: 10.1002/sia.1195

SIA

Adsorption of alginic acid to titanium investigated using x-ray photoelectron spectroscopy and atomic force microscopy†

Robert A. Brizzolara*

Naval Surface Warfare Center, Code 645, 9500 MacArthur Blvd, West Bethesda, MD 20817-5700, USA

Received 11 July 2001; Revised 7 September 2001; Accepted 20 November 2001

X-ray photoelectron spectroscopy (XPS) and atomic force microscopy (AFM) have been used to characterize the adsorption of alginic acid to titanium as a function of alginic acid solution pH. It was found that alginic acid adsorbs in greater quantity at acidic pH than at basic pH. The results provide evidence for an anion-exchange adsorption mechanism at weakly acidic pH. Addition of calcium chloride to the alginic acid solution results in a reduction of alginic acid adsorption at acidic pH and an increase at basic pH. This behavior can be explained by inhibition of anion exchange by the calcium cation at acidic pH and mediation of a bond between alginic acid and the titanium surface at basic pH. Elucidation of the adsorption chemistry of biofilm components to the surfaces of engineering materials is a prerequisite to developing surface modification strategies to reduce biofouling adhesion. Data presented herein can be used in the future as a baseline for comparison with data for such modified surfaces. Published in 2002 John Wiley & Sons, Ltd.

KEYWORDS: alginic acid; titanium; x-ray photoelectron spectroscopy; atomic force microscopy; biofilm

INTRODUCTION

Biological fouling (biofouling) is a chronic and costly problem in the maritime industry. Biofouling in cooling systems results in higher operating temperatures and decreased efficiency. The heat-transfer surfaces in these cooling systems cannot be treated with anti-fouling coatings because this would increase the heat-transfer resistance to an unacceptable level. Chlorination is commonly used for fouling control in seawater systems such as piping and heat exchangers; however, environmental regulations on chlorine discharges are forcing alternative approaches to be considered. Ideally, such an approach would be capable of controlling biofouling in a cost-effective way without resulting in the storage or discharge of hazardous chemicals. Such approaches might include modifying surfaces that are prone to biofouling to produce a surface with lower fouling adhesion. A prerequisite for such a surface modification approach is an improved understanding of the adhesion of biofouling to a surface.

The objective of this work is to develop an improved understanding of the chemical interaction between alginic acid and a titanium surface. Alginic acid is a major component of bacterial extracellular polysaccharides and titanium is a commonly used material in shipboard heat exchangers. Atomic force microscopy (AFM) and X-ray photoelectron spectroscopy (XPS) have been used to examine alginic acid adsorption to a titanium surface. Information regarding chemical change in the alginic acid resulting from its adsorption to titanium is elucidated.

The nature of the metal surface determines the availability of chemical groups for adhesion reactions with biological material. The titanium surface spontaneously forms an oxide (TiO_2) of thickness ~3 nm in the ambient. If the surface is exposed to water, the outermost TiO_2 layer hydroxylates, resulting in two distinct hydroxyl groups, one acidic and one basic.[1–3] The basic hydroxyl group is singly coordinated and can be exchanged by other anions in acidic milieu.[1–3] The acidic hydroxyl group is doubly coordinated and is expected to interact with cations at basic pH.[1–3] The net charge on the surface is zero at a pH that is the average of the p*K* values for the acidic and basic hydroxyl groups. Measurements of this isoelectronic point (IEP) range between 5 and 6 for the titanium surface.[4,5]

Alginic acid is a polysaccharide composed of a linear polymer of mannosyluronic and glucolosyluronic acids.[6] It contains carboxyl and hydroxyl groups that potentially can interact with the hydroxylated titanium surface. The carboxyl group potentially can interact with the surface via an anion-exchange reaction or by hydrogen bonding. The hydroxyl group may interact via hydrogen bonding. The p*K* of the carboxyl group is ~3.[7]

There is work in the literature concerning the adsorption of biofilm components to surfaces. X-ray photoelectron

*Correspondence to: R. A. Brizzolara, Naval Surface Warfare Center, Code 645, 9500 MacArthur Blvd, West Bethesda, MD 20817-5700, USA. E-mail: BrizzolaraRA@nswccd.navy.mil
Contract/grant sponsor: NSWC (Naval Surface Warfare Center).

spectroscopy studies of copper thin films immersed in gum arabic, bacterial culture supernatant and *Pseudomonas atlantica* showed that gum arabic resulted in Cu(II), bacterial culture supernatant in Cu(I) and *P. atlantica* in Cu(0).[8] Chemical changes in the biological material due to adsorption to the copper surface were not identified. The adsorption of mussel adhesive protein (MAP) to the surface of polystyrene and polyoctadecylmethacrylate (POMA) has been investigated using XPS.[9] The authors concluded that MAP adsorbed to polystyrene through $\pi-\pi$ or cation$-\pi$ interactions between aromatic or lysine residues on MAP and the polystyrene surface. No protein–surface functional group interactions were observed between MAP and POMA. This leads to protein–protein interactions being favored over protein–surface interactions and results in aggregation of proteins on the surface.

There is work in the literature on the adsorption of amino acids to titanium as a function of pH from sodium chloride solution and related acid–base interactions.[10,11] It was found that methionine and alanine do not adsorb in detectable quantities at any pH. The other amino acids examined (cysteine, proline, glycine, serine, tryptophan, aspartic acid, glutamic acid and lysine) adsorb only in acidic milieu. An exchange reaction between the carboxyl group of the amino acid and the basic surface hydroxyl group was proposed as the attachment mechanism. It is not clear what it is about alanine and methionine that causes them not to adsorb to titanium.

In the present work, AFM and XPS have been used to investigate the adhesion of alginic acid to titanium as a function of alginic acid solution pH and the resulting acid–base interactions between adsorbate and substrate. Varying the pH gives information regarding the different charge states of the ionizable groups on the hydroxylated titanium surface and alginic acid adsorbate. X-ray photoelectron spectroscopy has been used to quantify the alginic acid adsorbed to titanium. Additionally, information in the XPS spectra has been used to elucidate chemical changes in the alginic acid due to adsorption to the titanium surface and the thickness of the alginic acid layer. Atomic force microscopy images have been used to characterize the morphology and thickness of the adsorbed alginic acid layer. Thin films of adsorbed hexanoic acid and glucose also were investigated in order to separate the effects of the carboxyl chemistry from those of the hydroxyl chemistry.

EXPERIMENTAL

High-purity (>99.99%) titanium foils (Alfa-Aesar, Ward Hill, MA) were cut into pieces ~13 mm × 13 mm and cleaned ultrasonically in electronic-grade acetone for at least 1 h and then in methanol for at least 15 min. The foils were dried using flowing dry nitrogen. The following solutions were prepared: 2% (w/v) alginic acid sodium salt (Sigma A-2158), 2% (w/v) alginic acid sodium salt plus 2% (w/v) calcium chloride (Sigma C-3881), 2% (w/v) hexanoic acid sodium salt (Sigma C-4026) and 2% (w/v) glucose (Sigma G-7528). The pH was adjusted to the desired value by addition of HCl or NaOH. The clean titanium foils were immersed in the alginic acid, hexanoic acid or glucose solution within a few minutes after cleaning. Immersion times were ~22–26 h. The foils then were removed from the solutions and rinsed thoroughly with deionized water to remove unadsorbed material. The foils were dried using flowing dry nitrogen. The foils were analyzed within a few days of removal from solution. Bulk powders of alginic acid, hexanoic acid and glucose were prepared for XPS analysis by pressing them onto an indium foil using a pressure of 4000 lb in^{-2} for several minutes.

The AFM images were used to assess the uniformity and thickness of alginic acid coverage on titanium. This information was used subsequently to aid in interpreting the XPS data. The XPS spectra of alginic acid adsorbates were used to assess the chemical interaction between alginic acid and the titanium surface and to determine the thickness of the adsorbate layer. Additionally, XPS spectra of hexanoic acid and glucose adsorbed onto titanium at various pHs were used to separate effects of the hydroxyl functionality from the carboxyl functionality on the adsorption behavior. These were for comparison to the alginic acid adsorbate spectra. In addition, XPS spectra were obtained for bulk alginic acid, hexanoic acid and glucose powders that had been pressed into an indium foil. Finally, XPS spectra were acquired of the clean titanium surface with no adsorbate, for comparison purposes. These clean titanium foils were prepared using the same procedure as the alginic acid adsorbates except that they were immersed in deionized water at pH values of 1.5, 7.0 and 12.5.

Atomic force microscopy was performed using a Digital Instruments Nanoscope II with a revision 3 head. Both the D-scanner and J-scanner were used, along with 200 μm cantilevers. The $x-y$ calibration was performed using the 1 μm pitch (D-scanner) and 10 μm pitch (J-scanner) calibration gratings supplied with the instrument. Additionally, the tip was characterized periodically using a 2.12 μm pitch calibration grating (Model TGT01 NT-MDT POB 50, Moscow 103305, Russia). If degradation was observed in the AFM image of the calibration grating, the tip was replaced immediately. At least three points on each sample were analyzed. Additionally, the AFM tip was used to remove the alginic acid adsorbate from a selected area to obtain an estimate of adsorbate thickness. A similar procedure has been described previously.[12] The sample was raised toward the AFM tip by 3–10 μm, thereby increasing the tip–sample force. Using this increased force, the tip was rastered over a 1–10 μm area for ~10 frames, removing the adsorbate from that portion of the surface. The sample then was lowered away from the tip, re-establishing a normal tip–sample force. An image was acquired of the etched area. The thickness of the adsorbate was determined by measuring the depth of the indentation. Control samples of clean titanium foil and titanium foil with thicker organic coatings also were analyzed using this procedure, to ensure that the appropriate tip–sample force was used.

The XPS was performed using a Physical Electronics 5400 spectrometer with a photoelectron take-off angle of 45°. A monochromatic aluminum x-ray source operating at 400 W was used to acquire survey and multiplex spectra for the adsorbate samples. These samples were used to

determine carbon and organic oxygen atomic concentrations. Additionally, survey spectra acquired of the adsorbate samples using an unmonochromated magnesium source were used to determine C 1s and C KVV peak intensities for layer thickness determination. The unmonochromated magnesium source also was used to acquire spectra of bulk alginic acid, hexanoic acid and glucose in order to minimize sample charging. The pass energy for the survey spectra was 179 eV and for the high-resolution spectra was 17.9 eV. A 1 × 3 mm analysis area was employed. The base pressure of the system was 2×10^{-9} Torr and the pressure during the analysis was $\sim 2 \times 10^{-8}$ Torr. The XPS energy scale was calibrated and linearized using a 99.9985% copper foil (Alfa-Aesar, Ward Hill, MA) that had been sputtered *in situ* for several minutes. The position of the Cu $2p_{3/2}$ peak was set at 932.7 eV and the position of the Cu 3p peak was set to 75.0 eV. Atomic concentrations of the elements present in the samples were determined from survey spectra using elemental sensitivity factors provided in the Physical Electronics software.

Relative concentrations of different chemical states of carbon and oxygen were determined using curve fitting. A linear background and Gaussian peak shapes were employed. Carbon curve fits were performed using the Physical Electronics software. Three carbon components were used in the fits: $(CH_2)_n$, carbon bound to one oxygen atom and a component that included both carboxyl and carbon bound to two oxygen atoms. The separation of the three carbon components in the raw data was sufficient so that the initial peak positions for the fit could be determined visually. Curve fits on the O 1s high-resolution data were performed using PeakFit, version 4 (SPSS Inc., Richmond, CA). Three components were assumed in the fit conditions: oxide, carbonyl and a component that included both hydroxyl and glycosidic oxygen. Initial peak positions of the two organic oxygen components (carbonyl and hydroxyl/glycosidic) could not be determined visually due to the small binding energy separation, therefore the initial peak positions of all three components were determined from the minimum in the second derivative of the spectrum.

The XPS results presented in this paper reflect the carbon and organic oxygen concentrations due to the adsorbate. For alginic acid and glucose, the carbon atomic concentration is that of carbon bound to one oxygen atom plus carbon bound to two oxygen atoms plus carboxyl carbon. The $(CH_2)_n$ carbon component was excluded from this part of the analysis because it is not present in alginic acid or glucose. For hexanoic acid, the carbon atomic concentration is that of carbon bound to one oxygen atom plus carboxyl carbon plus $(CH_2)_n$. The organic oxygen atomic concentration for alginic acid, glucose and hexanoic acid is the sum of the carbonyl oxygen concentration and hydroxyl/glycosidic oxygen concentration. The oxygen signal due to the metal oxide has been excluded from the analysis. The XPS survey spectra also were used to estimate the thickness of the adsorbate layer. This was accomplished using the intensities of the C 1s and C KVV peaks, corrected for the substrate photoelectron-generated C KVV electrons in the alginic acid layer. This procedure has been described previously.[13,14]

Advancing contact angle measurements were performed by placing a 1–2 μl drop of deionized water on the sample surface and immediately measuring the contact angle (Kayness Model D1060 contact angle viewer, Morgantown, PA). The contact angles reported in this paper are the averages of measurements at three different points on each sample.

RESULTS

Clean titanium foils

Clean titanium foils immersed in deionized water at pH 1.5, 7.0 and 12.5 were analyzed using AFM and XPS. These samples served as controls for the adsorbate samples described below, establishing a background level of adventitious material present on the titanium foils that had not been immersed in alginic acid solution. The AFM images of these control samples appeared identical at all three pH values and revealed little discernable adventitious material. An example of these images is shown in Fig. 1. The image is of a 1 μm × 1 μm area and the height range is 50 nm. No evidence of low or high pH corrosion was observed.

High- and low-resolution XPS spectra were acquired of the control titanium foils. Seven clean foils immersed in water of pH 7 and two each at a pH of 1.5 and 12.5 were analyzed. Following immersion, the foils were rinsed and dried using the procedure described above and then placed in the spectrometer within a few seconds. Carbon, oxygen and titanium atomic percentages were determined for each foil from the low-resolution spectra. The C 1s peak components and the O 1s peak components associated with organic materials (not including the oxide component) were separated by peak-fitting the high-resolution data. The atomic percentages of carbon and organic oxygen were summed. Two values were obtained: one that includes $(CH_2)_n$, for comparison with hexanoic acid (which contains $(CH_2)_n$); and a value that does not include $(CH_2)_n$, for

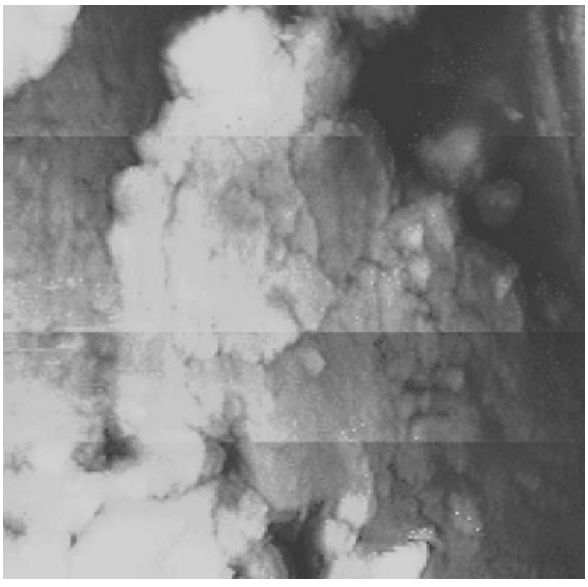

Figure 1. AFM image of a clean titanium foil. The image area is 1 μm × 1 μm, and the height range is 50 nm. Little adventitious material is seen.

comparison with alginic acid and glucose (which do not contain $(CH_2)_n$). The results are given in Table 1. For foils immersed in the pH 7 solution, the average value of carbon (including $(CH_2)_n$) plus organic oxygen is 43.3 ± 1.6 at.%. The average value of carbon (not including $(CH_2)_n$) plus organic oxygen is 24.9 ± 0.7 at.%. The values are slightly lower for the foils immersed in pH 1.5 and 12.5 solutions. These values can be considered as a background concentration of adventitious material for comparison with the data for alginic acid, glucose and hexanoic acid adsorbates on titanium, described below. The errors stated in Table 1 represent the standard deviation of the mean determined from the seven samples for pH 7 and two samples each for pH 1.5 and 12.5.

Bulk powders

High- and low-resolution XPS spectra were acquired for bulk powders of alginic acid, hexanoic acid and glucose. These data were used as standards for comparison with the adsorbate data described below. The binding energies obtained from the bulk powders are given in Tables 2–4. These binding energies were used as a comparison with the binding energies determined from the peak fits for the alginic acid, hexanoic acid and glucose adsorbates, given in the right-hand columns of Tables 2–4. Note that the binding energies obtained for the adsorbates agree well with those obtained for the bulk powders. No changes in adsorbate binding energy as a function of pH were observed. Only one oxygen component is seen for the bulk hexanoic acid due to the equivalence of the carboxylate anion's oxygen ions.

The carbon/organic oxygen (not including the oxide component) atomic concentration ratio was determined from the bulk powder XPS data for alginic acid, hexanoic acid and glucose. The $(CH_2)_n$ signal was not included in this ratio for alginic acid and glucose because these compounds do not contain $(CH_2)_n$ but it was included in the ratio for hexanoic acid. These values are compared with the theoretical values in Table 5.

Table 1. Background levels of carbon plus organic oxygen atomic percentages for control titanium foils

	C + O $(CH_2)_n$	C + O $(CH_2)_n$
1.5	37.5 ± 1.8	23.4 ± 1.5
7.0	43.3 ± 1.6	24.9 ± 0.7
12.5	32.8 ± 1.7	18.8 ± 0.3

Table 2. Binding energies for alginic acid bulk powder and thin films

	Bulk powder binding energy (eV)	Thin-film average binding energy (eV)
C–O	286.2	286.1
Carboxyl C and O–C–O	287.7	288.0
O–Ti oxide	—	529.6
Carbonyl O	531.3	531.2
Hydroxyl/glycosidic O	532.9	532.5

Table 3. Binding energies for hexanoic acid bulk powder and thin films

	Bulk powder binding energy (eV)	Thin-film average binding energy (eV)
$(CH_2)_n$ carbon	284.6	284.6
C–O	—	286.0
Carboxyl C	288.0	288.2
O–Ti oxide	—	529.6
Carbonyl O	531.3	531.5
Hydroxyl O	—	532.9

Table 4. Binding energies for glucose bulk powder and thin films

	Bulk powder binding energy (eV)	Thin-film average binding energy (eV)
C–O	286.3	286.1
O–C–O	287.9	288.2
O–Ti oxide	—	529.7
Hydroxyl/glycosidic O	532.6	532.6

Table 5. Carbon/organic oxygen ratios: measured and theoretical values

	Measured value	Theoretical value
Bulk alginic acid	0.9	1.0
Bulk hexanoic acid	2.8	3.0
Bulk glucose	0.9	1.0
Clean Ti (not incl. HC/incl. HC), pH 7	$0.7 \pm 0.1/1.9 \pm 0.1$	—
Clean Ti (not incl. HC/incl. HC), pH 1.5	$0.7 \pm 0.1/1.8 \pm 0.1$	—
Clean Ti (not incl. HC/incl. HC), pH 12.5	$0.6 \pm 0.1/1.8 \pm 0.2$	—

Alginic acid adsorbate on titanium

Figure 2 is an AFM image of a titanium foil that had been immersed in a 2% solution of alginic acid at pH 12.7. This surface has a similar morphology to the titanium foil immersed in water shown in Fig. 1, indicating that little alginic acid has adsorbed to this surface. Figure 3 is an AFM image of a titanium foil that had been immersed in a 2% solution of alginic acid at a pH of 2.2. The surface morphology in Fig. 3 is different from that in Figs 1 and 2 and indicates the presence of an overlayer on the titanium. The overlayer appears to cover the entire surface but is non-uniform in thickness.

Some regions of the titanium surface are covered by approximately spherically shaped features interpreted as agglomerates of alginic acid. The spheres range in diameter from tens to hundreds of nanometers. Other regions of the surface are covered with a thinner layer that can be

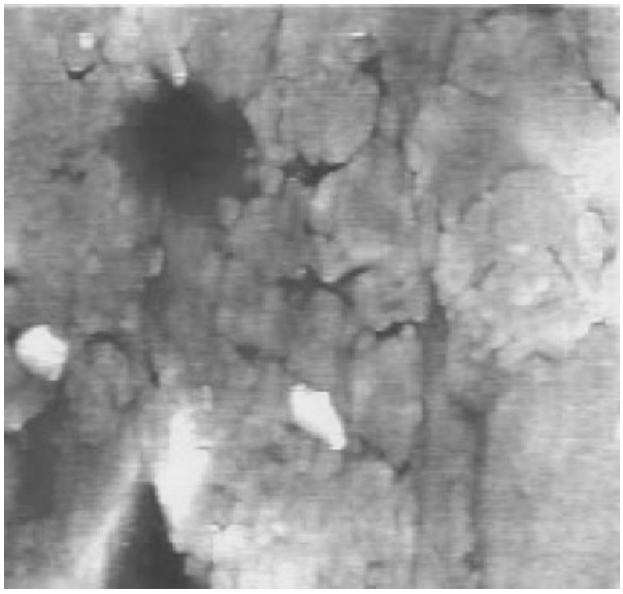

Figure 2. AFM image of a titanium foil immersed in alginic acid solution of pH 12.7. Little alginic acid adsorbate can be seen. The image area is 1 μm × 1 μm, and the height range is 50 nm.

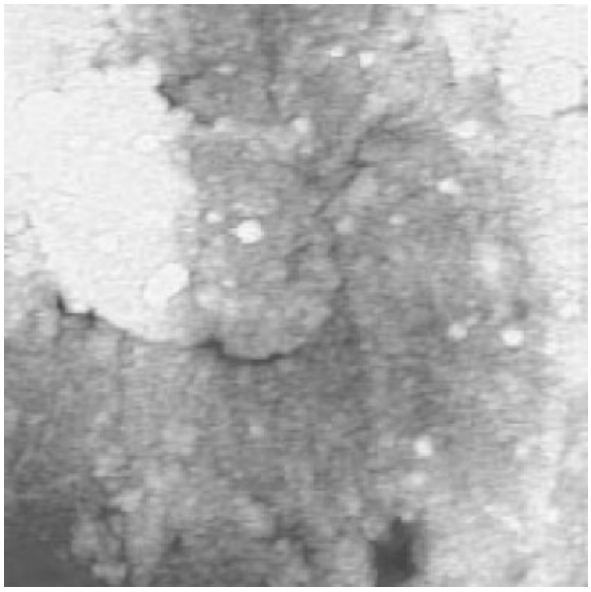

Figure 3. AFM image of a titanium foil immersed in alginic acid solution at pH 2.2. Alginic acid adsorbate completely covers the surface with a non-uniform thickness. The image area is 1 μm × 1 μm, and the height range is 50 nm.

differentiated from the clean titanium surface in Figs 1 and 2 by its texture. Images of a titanium sample immersed in alginic acid solution at a pH of 5.5 appear similar to the pH 2.2 sample. Thus, the AFM images show that there is an alginic acid overlayer present on the titanium surface at acidic pH and less alginic acid is adsorbed to titanium at basic pH.

Figure 4 is an AFM image of a titanium foil immersed in alginic acid at pH 2.2 for ~24 h. Prior to acquiring this image, the AFM tip was used to etch away the alginic acid coating, according to the procedure given in the previous section. The

Figure 4. AFM image of a Ti foil immersed in alginic acid at a pH of 2.2. A higher magnification image (Fig. 3) showed complete coverage of the surface by alginic acid. In this figure, an AFM tip was used to etch away the alginic acid coating so that the thickness of the alginic acid layer could be determined by measuring the depth of the crater. The depth of the crater was determined to be 0–10 nm.

image was viewed in cross-section to determine the depth of the etched area and thus of the alginic acid coating. The alginic acid thickness could not be measured precisely using this technique because the depth of the etched area was much less than the roughness of the titanium surface. However, it could be determined that the alginic acid thickness was <10 nm.

Figures 5 and 6 are XPS survey spectra of titanium foils that had been immersed in 2% alginic acid solution of pH 4.9 and 12, respectively, according to the procedure given in the previous section. The major peaks in the spectra are O 1s, Ti 2p and C 1s. The larger C 1s peak in Fig. 5 is consistent with the greater amount of alginic acid adsorbed at acidic pH as observed using AFM. The thickness of the alginic acid coating as a function of solution pH was

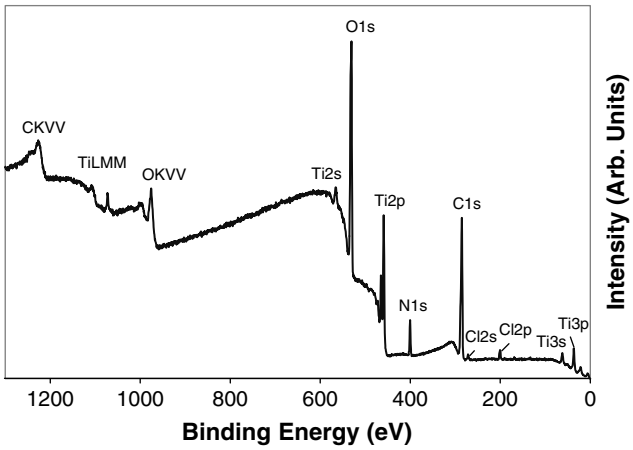

Figure 5. The XPS survey spectrum of a titanium foil immersed in alginic acid solution at pH 4.9. This sample has substantially more alginic acid adsorbed to it than the pH 12 sample of Figure 6, as evidenced by the larger carbon peak.

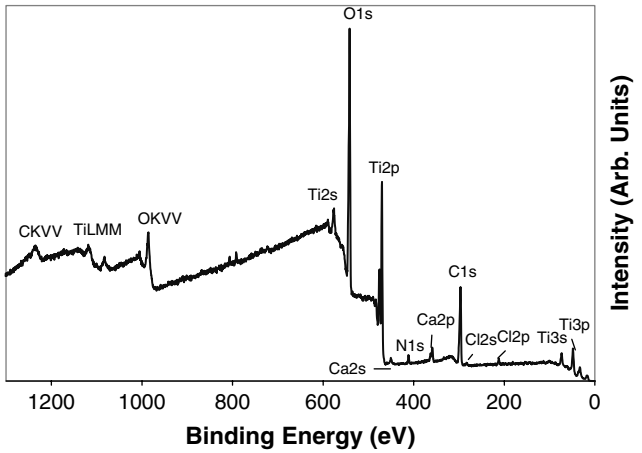

Figure 6. The XPS survey spectrum of a titanium foil immersed in alginic acid solution at pH 12. This sample has substantially less alginic acid adsorbed to it than the pH 4.9 sample of Fig. 5, as evidenced by the smaller carbon peak.

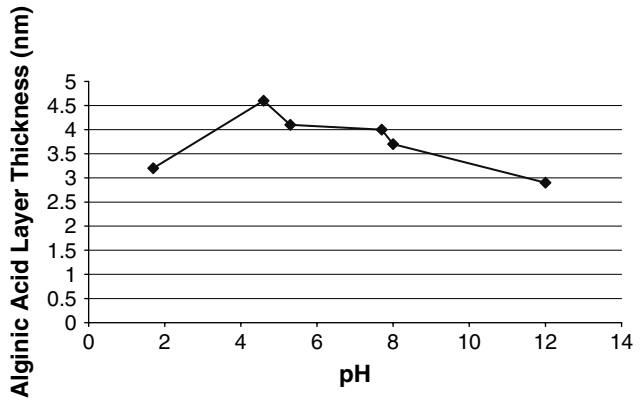

Figure 7. Plot of approximate thickness of alginic acid layer versus solution pH. Thicknesses were determined by the XPS C1s/C KVV method corrected for the substrate effect.

determined using XPS C 1s and C KVV peak intensities measured from the survey spectra, corrected for substrate photoelectron emission, as described in the previous section. This result is shown in Fig. 7. It is seen that the maximum layer thickness of ~4.5 nm occurs at a pH of ~4.5. The AFM images discussed previously showed that the alginic acid adsorbate had non-uniform thickness. The layer thickness value measured using XPS is an average value. It should be noted that the dependence of the C 1s to C KVV ratio on the layer thickness is very weak for layer thicknesses of $\gtrsim$3 nm, therefore the accuracy of the measurement in the weakly acidic region is degraded. Nevertheless, the XPS and AFM layer thickness results agree quite well.

High-resolution C 1s and O 1s XPS spectra were acquired of titanium foils that had been immersed in aqueous solutions of alginic acid at various pH values. One to three samples were analyzed at each pH. Examples of these spectra are plotted in Fig. 8 (C 1s) and Fig. 9 (O 1s). For the C 1s spectrum (Fig. 8) three components were assumed for the fit. The lowest binding energy component was assigned to $(CH_2)_n$, the middle component to carbon bound to a single oxygen atom and the highest component was used

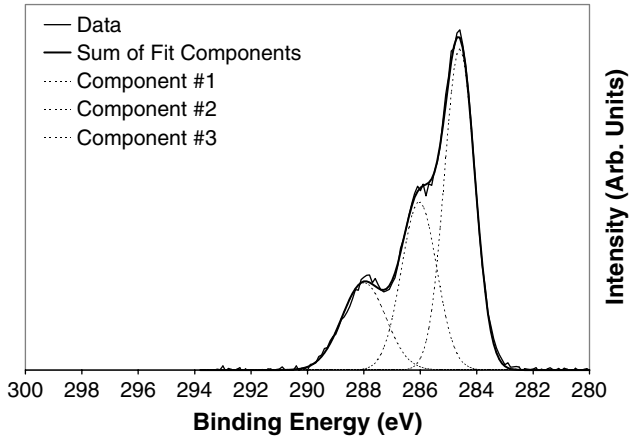

Figure 8. High-resolution spectrum of the curve-fit of the C 1s spectrum of a titanium foil immersed in alginic acid solution at pH 4.9. The spectrum was fit to three components. The subsequent analysis employed the two high-binding energy components that originated from the alginic acid.

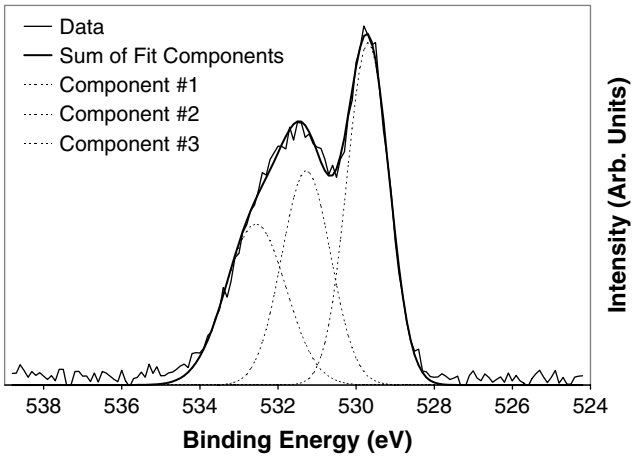

Figure 9. High-resolution spectrum of the curve-fit of the O 1s spectrum of a titanium foil immersed in alginic acid solution at pH 4.9. The spectrum was fit to three components. The subsequent analysis employed the two high-binding energy components that originated from the alginic acid.

to represent both carbon bound to two oxygen atoms and carboxylic carbon. Figure 9 shows the presence of two peaks in the O 1s spectrum: one at ~529.7 eV and a broad peak at ~531.5 eV. The O 1s spectra were fit to three components. The lowest binding energy component was assigned to titanium oxide, the peak at 529.7 eV. Two components were used to fit the high-binding-energy broad peak at 531.5 eV. This was based on the relatively large width of this peak, the chemical information in the C 1s spectrum and the number of components observed in the O 1s spectrum of bulk alginic acid (see Table 2). For the broad peak centered at 531.5 eV, the lower binding energy component was assigned to carbonyl oxygen and the higher binding energy component was used to represent both hydroxyl and glycosidic oxygen. Although the O 1s spectrum was fit to three components, it should be made clear that in the following analysis it was only necessary to resolve the oxide and organic components of this spectrum (i.e. the peak at 529.7 eV and the broad peak

centered at 531.5 eV). It was not necessary to resolve the carbonyl, hydroxyl and glycosidic components that comprise the broad organic oxygen peak, because the intensities of the two components used to represent these three chemistries were summed subsequent to the curve-fitting procedure.

To obtain information regarding the adsorption of alginic acid to the titanium surface, the atomic percentages of carbon and oxygen components associated with alginic acid were summed. This sum includes the middle- and high-binding-energy carbon components and the middle- and high-binding-energy oxygen components. The sum does not include the low-binding-energy carbon component $(CH_2)_n$ because alginic acid does not contain $(CH_2)_n$. The sum also does not include the low-binding-energy oxygen component that is due to titanium oxide. Figure 10 is a plot of the sum of the carbon and organic oxygen atomic percentages due to the alginic acid adsorbate versus solution pH. Figure 10 shows that the sum of the carbon and organic oxygen atomic percentages from the alginic acid adsorbate is ~35% at basic pH and increases to a maximum of 55% at a pH of 2. These values are greater than the values given in Table 1 for the control titanium foil immersed in water with no alginic acid adsorbate. The carbon/organic oxygen ratio due to the alginic acid adsorbate on titanium is plotted as a function of pH in Fig. 11. This quantity is determined from the same data as in Fig. 10. Figure 11 shows that the carbon/organic oxygen ratio is between 0.75 and 0.80 at pH > 11. It increases to 0.9 at pH 7–11 and increases further to a maximum of ~1.05 at a pH of 3.5. Thus, the carbon/organic oxygen ratio increases by 17% between pH 7–11 and pH 3.5. The carbon/organic oxygen ratio measured between pH 7 and 11 agrees well with the value of 0.9 measured for bulk alginic acid (see Table 5) and is greater than the value of 0.6–0.7 measured for the control titanium foil. The carbon/organic oxygen ratio at pHs > 11 agrees with the value measured for the control titanium foil.

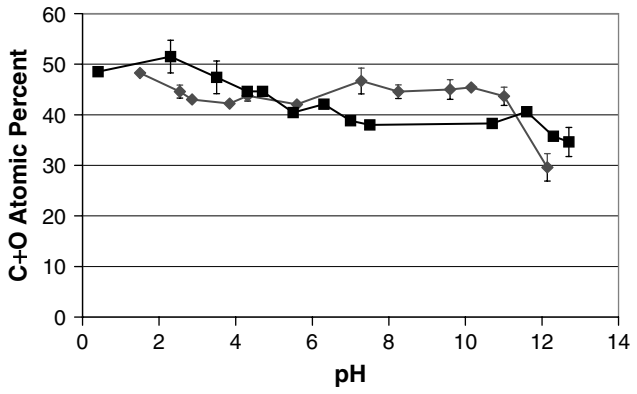

Figure 10. The sum of carbon and organic oxygen atomic percentages due to alginic acid adsorbed on titanium plotted versus solution pH. (■) without $CaCl_2$; (♦) with $CaCl_2$. The error bars represent the standard deviation of the mean of either two or three samples, with the exception of pH 4.7 for which only one sample was run. Points without error bars represent cases where the error bar was smaller than the size of the data point with the exception of the pH 4.7 data point.

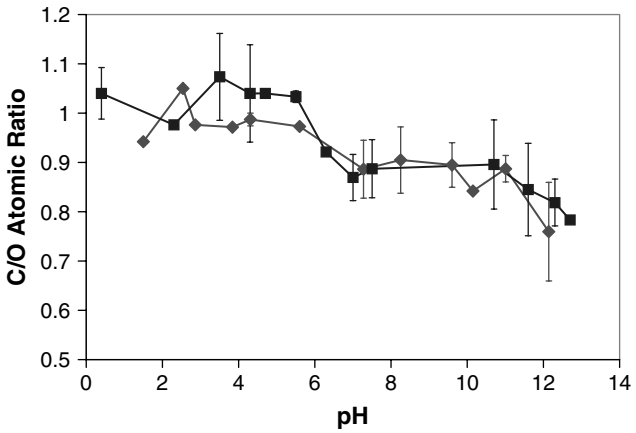

Figure 11. The ratio of carbon and organic oxygen atomic percentages due to alginic acid adsorbed on titanium plotted versus solution pH. (■) without $CaCl_2$; (♦) with $CaCl_2$. The error bars represent the standard deviation of the mean of either two or three samples, with the exception of pH 4.7 for which only one sample was run. Points without error bars represent cases where the error bar was smaller than the size of the data point, with the exception of the pH 4.7 data point.

Hexanoic acid and glucose adsorbates on titanium

To separate the effects of the carboxyl functionality from the hydroxyl functionality on the adsorption of alginic acid to titanium, high- and low-resolution XPS spectra were acquired of titanium foils that had been immersed in aqueous solutions of hexanoic acid and glucose at various pH values. Hexanoic acid contains the carboxyl functionality but not the hydroxyl, and glucose contains the hydroxyl functionality but not the carboxyl. The sum of the carbon and organic oxygen atomic percentages versus solution pH for hexanoic acid and for glucose is shown in Fig. 12. The $(CH_2)_n$ is included in the carbon atomic percentage for hexanoic acid but not for glucose. One to two samples were analyzed at each data point. The maximum atomic concentration for the hexanoic acid adsorbate on titanium is ~46 at.% and occurs at a pH of ~4.3. The concentration decreases to ~36 at.% at basic pH. The values at weakly acidic pH are slightly above the values measured for the control titanium foil given in Table 1. The values measured at acidic and basic pH are comparable to those measured for the control titanium foil given in Table 1. The minimum atomic concentration of glucose adsorbate on titanium is ~21 at.% at basic pH. The glucose atomic concentration varies between 25 and 30% over the rest of the pH range. These values are comparable to those obtained for clean titanium given in Table 1.

The carbon/organic oxygen ratio is plotted for hexanoic acid and glucose in Fig. 13. The $(CH_2)_n$ is included in the carbon atomic percentage for hexanoic acid but not for glucose. For hexanoic acid, this ratio increases from a value of ~1.5–2 to a maximum of 3.4 at a pH of ~4.9. These values compare with the ratios (given in Table 5) of 2.8 measured for bulk hexanoic acid and 1.8–1.9 for the control titanium foil. The ratio for glucose is quite constant over the entire pH range, varying between 0.5 and 0.7. This value compares with the ratio of 0.7 measured for bulk glucose and the value of 0.6–0.7 for the control titanium foil (given in Table 5).

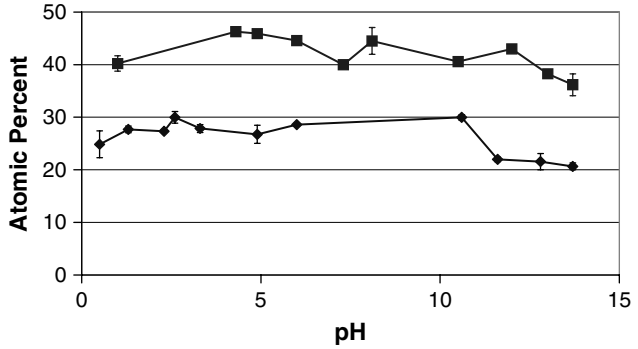

Figure 12. The sum of carbon and organic oxygen atomic percentages for hexanoic acid and glucose adsorbed on titanium plotted versus solution pH. The $(CH_2)_n$ is included in the carbon atomic percentage for hexanoic acid but not for glucose. (■) hexanoic acid. (♦) glucose. For hexanoic acid, the error bars represent the standard deviation of the mean of two measurements for pH 13, 7.0, 12, 8.1, 4.3 and 1. Points without error bars represent cases where the error bar was smaller than the size of the data point, except at pH 13, 10.5, 7.3, 6 and 4.9, for which only one sample was run. For glucose, the error bars represent the standard deviation of the mean of two measurements for all pH values except 2.3, for which only one sample was run. Points without error bars represent cases where the error bar was smaller than the size of the data point.

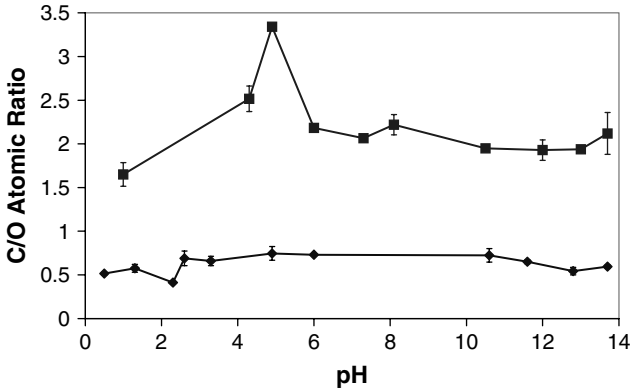

Figure 13. The ratio of carbon and organic oxygen atomic percentages due to hexanoic acid and glucose adsorbed on titanium plotted versus solution pH. The $(CH_2)_n$ is included in the carbon atomic percentage for hexanoic acid but not for glucose. (■) hexanoic acid. (♦) glucose. For hexanoic acid, the error bars represent the standard deviation of the mean of two measurements for pH 13, 7.0, 12, 8.1, 4.3 and 1. Points without error bars represent cases where the error bar was smaller than the size of the data point, except at pH 13, 10.5, 7.3, 6 and 4.9, for which only one sample was run. For glucose, the error bars represent the standard deviation of the mean of two measurements for all pH values except 2.3, for which only one sample was run. Points without error bars represent cases where the error bar was smaller than the size of the data point.

Contact angles were measured as a function of solution pH for the hexanoic acid adsorbate on titanium. These results are shown in Fig. 14. Each point represents the average of three measurements on that sample. Figure 14 shows that the maximum contact angle is 79° at a pH of 4.9, with substantial decreases at very acidic and very basic pH.

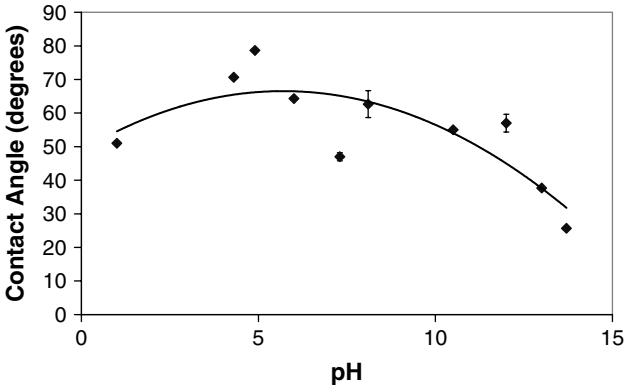

Figure 14. Contact angle as a function of pH for hexanoic acid on titanium. Three measurements were performed at each pH value. The error bars represent the standard deviation of the mean for the three measurements. Points without error bars represent cases where the error bar was smaller than the size of the data point.

X-ray photoelectron spectroscopy of alginic acid adsorbed to titanium in the presence of $CaCl_2$

High- and low-resolution XPS spectra were acquired of titanium foils that had been immersed in aqueous solutions of alginic acid and $CaCl_2$ at various pH values. Figure 10 is a plot of the sum of the carbon and organic oxygen atomic percentages due to the alginic acid adsorbate versus solution pH. This sum includes the carbon bonded to a hydroxyl group, carbon associated with the carboxyl group, carbonyl oxygen and hydroxyl oxygen. Note from this plot that the sum of the carbon and organic oxygen atomic percentages due to the alginic acid adsorbate is fairly constant as a function of pH. It varies between 43 and 48%, except at

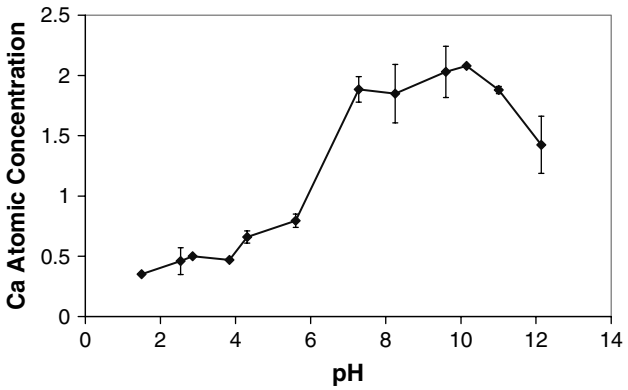

Figure 15. Calcium atomic concentration as a function of solution pH for alginic acid adsorbate on titanium from alginic acid/$CaCl_2$ solution. Two samples each were analyzed at pH values of 2.5, 4.3, 5.6, 7.3, 8.3, 9.6, 11.0 and 12.1. The error bars represent the standard deviation of the mean. Points without error bars represent cases where the error bar was smaller than the size of the data point, with the exception of the data points at pH values of 1.5, 2.9, 3.8 and 10.2 at which only one sample was analyzed.

very basic pH where it is lower. These values are greater than the values given in Table 1 for the control titanium foil with no alginic acid adsorbate. This behavior is different from the alginic acid adsorbed on titanium with no $CaCl_2$. The carbon/organic oxygen ratio due to the alginic acid adsorbed on titanium in the presence of $CaCl_2$ is plotted in Fig. 11. Figure 11 shows that the behavior of this ratio is different from that of alginic acid adsorbed on titanium with no $CaCl_2$. The carbon/organic oxygen ratio exhibits only a small increase going from basic to acidic pH. Figure 15 is a plot of calcium concentration on the titanium surface as a function of solution pH. This value is ~0.5 at.% at acidic pH and increases substantially to ~2 at.% at basic pH.

DISCUSSION

Comparison of Fig. 10 with the values for the control titanium foils given in Table 1 indicates that alginic acid adsorbs to titanium from deionized water at all pH values, but in greater quantities at acidic rather than basic pH. The maximum in the sum of carbon and organic oxygen atomic concentration occurs at a pH of 2.3. The XPS analysis indicates that the alginic acid layer thickness is a maximum at weakly acidic pH and the value in this pH range is ~4–4.5 nm. This layer thickness is an average value; the AFM image in Fig. 4 shows the alginic acid layer thickness to be non-uniform. A relatively small portion of the surface is covered by thicker alginic acid agglomerates and a larger fraction of the surface is covered by a thinner alginic acid overlayer. Control experiments consisting of immersion of titanium foils in water at pH 1.5, 7 and 12.5 (see Table 1) demonstrate that the maximum in alginic acid adsorption at weakly acidic pH is a real effect and not a result of excess adventitious material adsorbing at acidic pH.

Insight into the adsorption chemistry can be gained by examining the carbon/organic oxygen ratio as a function of pH (Fig. 11). This ratio exhibits a maximum of 1.05 at a pH of 3–5, which represents a 17% increase relative to basic pH. The measured increase in the carbon/oxygen ratio can be explained by an anion-exchange mechanism that is expected to occur at weakly acidic pH. At pH $\lesssim$ 3–5 the basic hydroxyl group on the titanium surface is protonated.[1–3]

$$\mathrm{Ti{-}OH + H^+ \Leftrightarrow Ti{-}OH_2^+ \Leftrightarrow Ti^+ + H_2O} \qquad (1)$$

At pH $\gtrsim$ 3 the carboxyl group on alginic acid is deprotonated

$$\mathrm{RCOOH \Leftrightarrow RCOO^- + H^+} \qquad (2)$$

The anion-exchange reaction can occur when the alginic acid carboxyl group is deprotonated and when the protonated hydroxyl group has dissociated from the titanium surface[1,3,10,11]

$$\mathrm{Ti{-}OH + RCOO^- + H^+ \Leftrightarrow Ti^+ + RCOO^- + H_2O \Leftrightarrow Ti{-}O{-}(C{=}O){-}R + H_2O} \qquad (3)$$

This occurs in a pH range from ~3 on the low side to 3–5 on the high side. Thus, immersion of titanium in acidic solutions results in dehydroxylation of the titanium surface. If the sample subsequently is rinsed with water, it rehydroxylates. However, if alginic acid reacts with the surface via anion exchange prior to the water rinse, then the titanium atoms on the surface that participate in the anion-exchange reactions with alginic acid are prevented from rehydroxylating. Referring to the right-hand side of Eqn. (3), one of the oxygen atoms of alginic acid's carboxyl group is now bound to a titanium atom. The binding energy of this oxygen atom is lower relative to an oxygen atom not bound to titanium. This oxygen atom then is included in the oxide peak rather than the organic oxygen peak during the curve-fit analysis. This manifests itself in the XPS data as a loss of one oxygen atom per alginic acid molecule adsorbed via anion exchange, relative to an alginic acid molecule adsorbed by an interaction other than anion exchange. Thus, because there are six oxygen atoms per alginic acid molecule, Eqn. (3) implies that a 17% increase in the carbon/organic oxygen ratio is expected in the case of anion exchange relative to the case of no anion exchange. This is in agreement with the increase in the carbon/organic oxygen ratio of 17% measured using XPS (Fig. 11). Alginic acid adsorption at other pH values is likely due to various modes of hydrogen bonding.

The measured 17% increase in the carbon/organic oxygen ratio for alginic acid adsorbed to titanium at weakly acidic pH indicates that most of the titanium surface is covered with a monolayer of alginic acid. If the coverage were greater than one monolayer, the measured increase in the carbon/organic oxygen ratio would be <17% due to the attenuation of O 1s photoelectrons from the alginic acid/titanium interface. A monolayer of alginic acid coverage suggests a layer thickness less than the 4.5 nm obtained using the XPS C 1s/C KVV method. However, it should be remembered that the areas of the surface covered with alginic acid agglomerates (shown in Fig. 3) increases the layer thickness obtained with the XPS C 1s/C KVV method. If the fractional coverage of the surface by these agglomerates is small, an increase of 17% in the carbon/organic oxygen ratio is reasonable, given the approximate nature of the XPS C 1s/C KVV method.

Further evidence for the anion-exchange reaction at weakly acidic pH is obtained by examining adsorbates of hexanoic acid and glucose on titanium. Analysis of adsorbates of these compounds separates the effects of the carboxyl group and the hydroxyl group on the adsorption. In the case of glucose and the hydroxyl group, the carbon and organic oxygen sum plotted in Fig. 12 is practically the same as the values obtained for the control titanium foils given in Table 1. This indicates that little glucose adsorbs to the surface at any pH. Furthermore, it is seen in Fig. 13 that no peak is evident in the carbon/organic oxygen ratio at weakly acidic pH. This indicates that anion exchange does not take place, as expected, because there is no carboxyl functionality in glucose. In contrast, although the carbon and organic oxygen sum values are not much different for the samples with adsorbed hexanoic acid than for the titanium control samples, there is a clear peak at a pH of 4.9 in the carbon/organic oxygen ratio. The peak value is a factor of ~1.7 greater than the values at other pH and the value

measured for bulk hexanoic acid. This is in agreement with the factor of 2 expected for anion exchange based on the carbon/oxygen ratio in hexanoic acid. The factor of two arises from the fact that the carbon/oxygen ratio in hexanoic acid changes from 6 : 2 to 6 : 1 after anion exchange, because on the right side of Eqn. (4) the oxygen atom bound to titanium is no longer counted as an organic oxygen during the curve-fitting procedure

$$\mathrm{Ti{-}OH + CH_3(CH_2)_4COOH \Leftrightarrow Ti{-}O{-}(C{=}O)(CH_2)_4CH_3 + H_2O} \quad (4)$$

The pH value of 4.9, at which the maximum hexanoic acid adsorption occurs, agrees with the pH value at which the maximum contact angle is measured (see Fig. 14). These results suggest that a thin layer of hexanoic acid has adsorbed to the titanium surface at weakly acidic pH and that the adsorption is via anion exchange. Furthermore, the contact angle data indicate that the maximum number of hexanoic acid $(CH_2)_n$ tails exposed to the solid/air interface occurs at weakly acidic pH. Therefore, the experimental evidence is consistent with an anion-exchange reaction that is responsible for alginic acid adsorption from deionized water at weakly acidic pH. It is likely that various modes of hydrogen bonding are responsible for hexanoic acid adsorption at other pH values.

In order to determine the effects of ions on the adsorption of alginic acid to titanium, the same experiments were performed with 2% $CaCl_2$ in solution. The results show that $CaCl_2$ significantly changes the adsorption behavior of alginic acid on titanium. Figure 10 shows that the presence of $CaCl_2$ results in less alginic acid adsorption at acidic pH and more alginic acid adsorption at basic pH. Figure 11 shows that at acidic pH the $CaCl_2$ has suppressed the anion-exchange reaction: there is only a small increase in carbon/oxygen at acidic pH in the presence of $CaCl_2$. The Ca^{2+} cation associates with the carboxylate anion in solution, inhibiting the anion-exchange reaction. At basic pH the increase in alginic acid adsorption can be understood in terms of a Ca^{2+} cation-mediated bond between the negatively charged carboxylate on alginic acid and the negatively charged deprotonated surface hydroxyl groups. This hypothesis is supported by the increase in calcium concentration at basic pH measured by XPS, depicted in Fig. 15. Cation-mediated adsorption of proteins to surfaces has been observed previously.[15]

CONCLUSIONS

Both XPS and AFM analyses have been used to investigate the adsorption chemistry of alginic acid to titanium from aqueous solutions at various pH values. Both the AFM and XPS results show that alginic acid adsorbs to titanium from deionized water in greater quantities at acidic pH than at basic pH. The AFM results show that the adsorbate completely covers the titanium surface at acidic pH, although the thickness is non-uniform. The XPS results indicate that the anion-exchange reaction is responsible for increased adsorption at weakly acidic pH. Further evidence for the anion-exchange mechanism is obtained from the XPS results for hexanoic acid and glucose adsorbates. Finally, addition of $CaCl_2$ to the alginic acid solutions results in less alginic acid adsorption at acidic pH and more alginic acid adsorption at basic pH relative to the case of no $CaCl_2$. At acidic pH, the calcium cation would be expected to associate with the carboxylate anion in solution, inhibiting the anion-exchange reaction and reducing alginic acid adsorption to the surface. At basic pH, the calcium cation most likely mediates a bond between the carboxylate anion and negatively charged surface oxygen species.

Elucidation of the adsorption chemistry of biofilm components to the surfaces of engineering materials is a prerequisite to developing surface modification strategies in order to reduce biofouling adhesion. The data presented herein can be used in the future as a baseline for comparison with data for such modified surfaces.

Acknowledgements

Many thanks are due to Dr Bruce Beard and Dr Jagadish Sharma for their valuable comments and insights. The NSWC Carderock Division In-House Laboratory Independent Research Program provided funding for this work.

REFERENCES

1. Boehm H. *Discuss Faraday Soc.* 1971; **52**: 264.
2. Parfitt G. *Prog. Surf. Membr. Sci.* 1976; **11**: 181.
3. Schindler P. In *Metal Ions in Biological Systems*, Sigel H (ed.). Marcel Dekker: New York, 1984; 108.
4. Parks G. *Chem. Rev.* 1965; **65**: 177.
5. Simmons GW, Beard BC. *J. Phys. Chem.* 1987; **91**: 1143.
6. Budavari S. *The Merck Index*. (11th edn) Merck: Rahway, NJ, 1989.
7. Stryer L. *Biochemistry* (4th edn). W.H. Freeman: New York, 1995; 23.
8. Jolley J. *Appl. Surf. Sci.* 1989; **37**: 469.
9. Baty A. *Langmuir* 1997; **13**: 5702.
10. Gold J, Schmidt M, Steinemann S. *Helv. Phys. Acta* 1989; **62**: 246.
11. Schmidt M, Steinemann S. *Fresenius J. Anal. Chem.* 1991; **341**: 412.
12. Brizzolara R. *Biosenso. Bioelectron.* 2000; **15**: 63.
13. Brizzolara R, Beard B. *Surf. Interface Analy.* 1999; **27**: 716.
14. Ebel M, Schmid M, Ebel H, Vogel A. *J. Electron. Spectrosc.* 1984; **34**: 313.
15. van Dulm P, Norde W, Lyklema J. *J. Coll. Interface Sci.* 1981; **82**: 77.